# Diamond Lattice in Single-component Molecular Crystals Comprising Tetrabenzoporphyrin Neutral Radicals

Kosuke Mine,[a] Sachie Arae,[a] Hiroshi Murakawa,[b] Masahisa Tsuchiizu,[c] Noriaki Hanasaki [b] and Masaki Matsuda *[a]

[a] Department of Chemistry, Kumamoto University, 2-39-1 Kurokami, Chuo-ku, Kumamoto 860-8555, Japan. E-mail: masaki@kumamoto-u.ac.jp

[b] Department of Physics, Osaka University, 1-1 Machikaneyama, Toyonaka, Osaka 560-0043, Japan.

[c] Department of Physics, Nara Women's University, Kitauoyanishi-machi, Nara 630-8506, Japan..

## Contents

## Experimental details

### Synthetic procedures

$M^{II}$(tbp) was prepared as per the previously reported procedure.[1] An electrocrystallization cell equipped with a glass frit between two compartments was used for the electrolysis of Co(tbp) solution (8.9 mg, 0.016 mmol) with (*n*-$Bu_4N$)·CN (11.5 mg, 0.043 mmol) in *N*,*N*-dimethylformamide (35 mL). A 0.2–1.0 μA constant current was applied between two platinum electrodes immersed in the solution of each compartment for 3–4 weeks at 40 °C. Black prism-shaped crystals of $Co^{III}(tbp^{\bullet-})(CN)_2$ (3.5 mg, 0.0056 mmol, 35%) deposited on the anode surface during the current flow, and were harvested via filtration. A similar procedure using Fe(tbp) and $Ph_4P$·CN, and Mn(tbp) and $Ph_4P$·Cl yielded black prism-shaped crystals of $Fe^{III}(tbp^{\bullet-})(CN)_2$, and $Mn^{III}(tbp^{\bullet-})Cl_2$, respectively.

### Crystal structure determination

Crystal data for $M^{III}$(tbp)$(CN)_2$ (M = Co, Fe) and $Mn^{III}$(tbp)$Cl_2$ were collected at 293 K using an automated Rigaku SuperNova system with monochromated Mo-Kα radiation ($\lambda$ = 0.71073 Å). The structure was solved using a direct method with SHELXT-2014/5[2] and refined using a full-matrix least-squares technique with SHELXL-2018/1.[3] Anisotropic and isotropic thermal parameters were employed for non-hydrogen and hydrogen atoms, respectively. Crystallographic data were deposited at the Cambridge Crystallographic Data Centre (CCDC).

### Measurements

The electrical resistivity of Co(tbp)$(CN)_2$ was measured using a physical property measurement system from Quantum Design over 2–300 K temperature range with a four-probe technique under ambient and hydrostatic pressures. Gold wires were attached to the sample using gold paste. Hydrostatic pressure (0.35–2.4 GPa) was applied using a BeCu piston-cylinder cell with a pressure medium of DEMNUM S-20. The pressure was monitored using the manganin wire resistance.

Static magnetic susceptibility measurements of polycrystalline samples were performed using a magnetic property measurement system form Quantum Design , i.e., a superconducting quantum interference device (SQUID) under 0.01 or 1 T of static magnetic field over a 2–300 K temperature range. The core diamagnetism value was calculated as a sum of the Pascal's constants and used to correct the data.

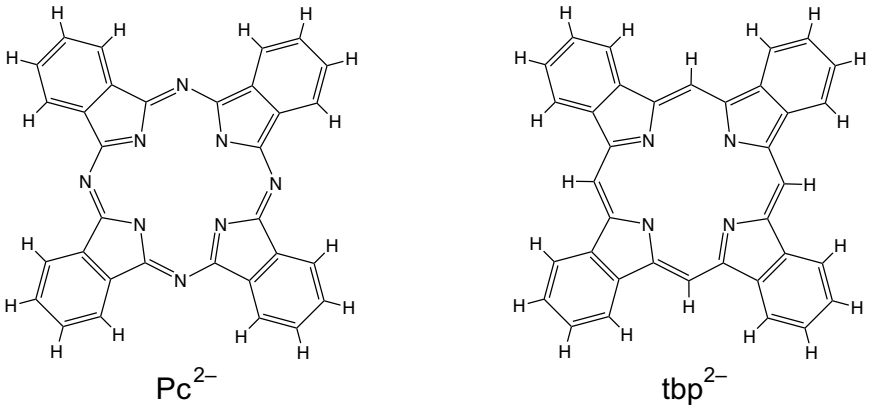


**Figure S1** Molecular structures of macrocyclic ligands of $Pc^{2-}$ (left) and $tbp^{2-}$ (right).

**Table S1.** Crystal data and structure refinement results for $Co(tbp)(CN)_2$, $Fe(tbp)(CN)_2$, and $Mn(tbp)Cl_2$.

| | | | |
|---|---|---|---|
| CCDC number | 2311221 | 2311222 | 2311223 |
| Chemical formula | $C_{38}H_{20}CoN_6$ | $C_{38}H_{20}FeN_6$ | $C_{36}H_{20}Cl_2MnN_4$ |
| Formula weight | 619.53 | 616.45 | 634.40 |
| Crystal description | Black prism | Black prism | Black prism |
| Temperature / K | 293 | 293 | 293 |
| Crystal system | Tetragonal | Tetragonal | Tetragonal |
| Space group | $I4_1/a$ | $I4_1/a$ | $I4_1/a$ |
| $a$ / Å | 13.6416(3) | 13.7275(3) | 13.7890(4) |
| $c$ / Å | 14.5402(6) | 14.5027(7) | 14.4334(8) |
| $V$ / Å$^3$ | 2705.83(16) | 2732.95(18) | 2744.3(2) |
| $Z$ | 4 | 4 | 4 |
| $d_{cal}$ / (g cm$^{-3}$) | 1.521 | 1.498 | 1.535 |
| Radiation wavelength / Å | 0.71073 (MoKα) | 0.71073 (MoKα) | 0.71073 (MoKα) |
| $\mu$ / mm$^{-1}$ | 0.677 | 0.594 | 0.711 |
| No. of measured reflections | 4041 | 4095 | 6430 |
| No. of independent reflections | 1574 | 1586 | 1589 |
| No. of observed reflections | 1334 ($I > 2\sigma(I)$) | 1220 ($I > 2\sigma(I)$) | 1181 ($I > 2\sigma(I)$) |
| $R$ ($I > 2\sigma(I)$) | $R_1 = 0.0357$ | $R_1 = 0.0404$ | $R_1 = 0.0379$ |
| | $wR_2 = 0.1010$ | $wR_2 = 0.1161$ | $wR_2 = 0.1199$ |
| Goodness-of-fit | 1.107 | 1.073 | 1.077 |
| Parameters | 103 | 103 | 98 |

The Gaussian 16 software package[4] was used to perform theoretical calculations using the density functional theory approach under the conditions of UB3LYP/6-311G(d) level. LANL2DZ basis set was applied for Mn, Fe, and Co atoms. Under the $D_{2d}$ symmetry, structural optimization and frequency analysis were performed on initial structure. The atomic coordinates obtained by crystal structure analysis were used as an initial structure.

| | Crystal | Optimized (open shell) |
|---|---|---|
| $Co(tbp)(CN)_2$ | 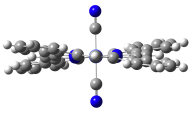 | 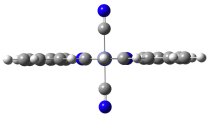 |
| $Fe(tbp)(CN)_2$ | 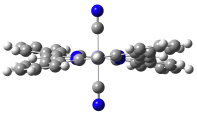 | 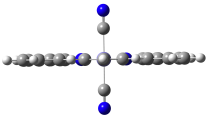 |
| $Mn(tbp)Cl_2$ | 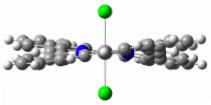 | 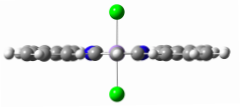 |

**Figure S2.** Molecular structures in crystals and optimized geometries by DFT theory of $Co(tbp)(CN)_2$, $Fe(tbp)(CN)_2$ and $Mn(tbp)Cl_2$ (side view).

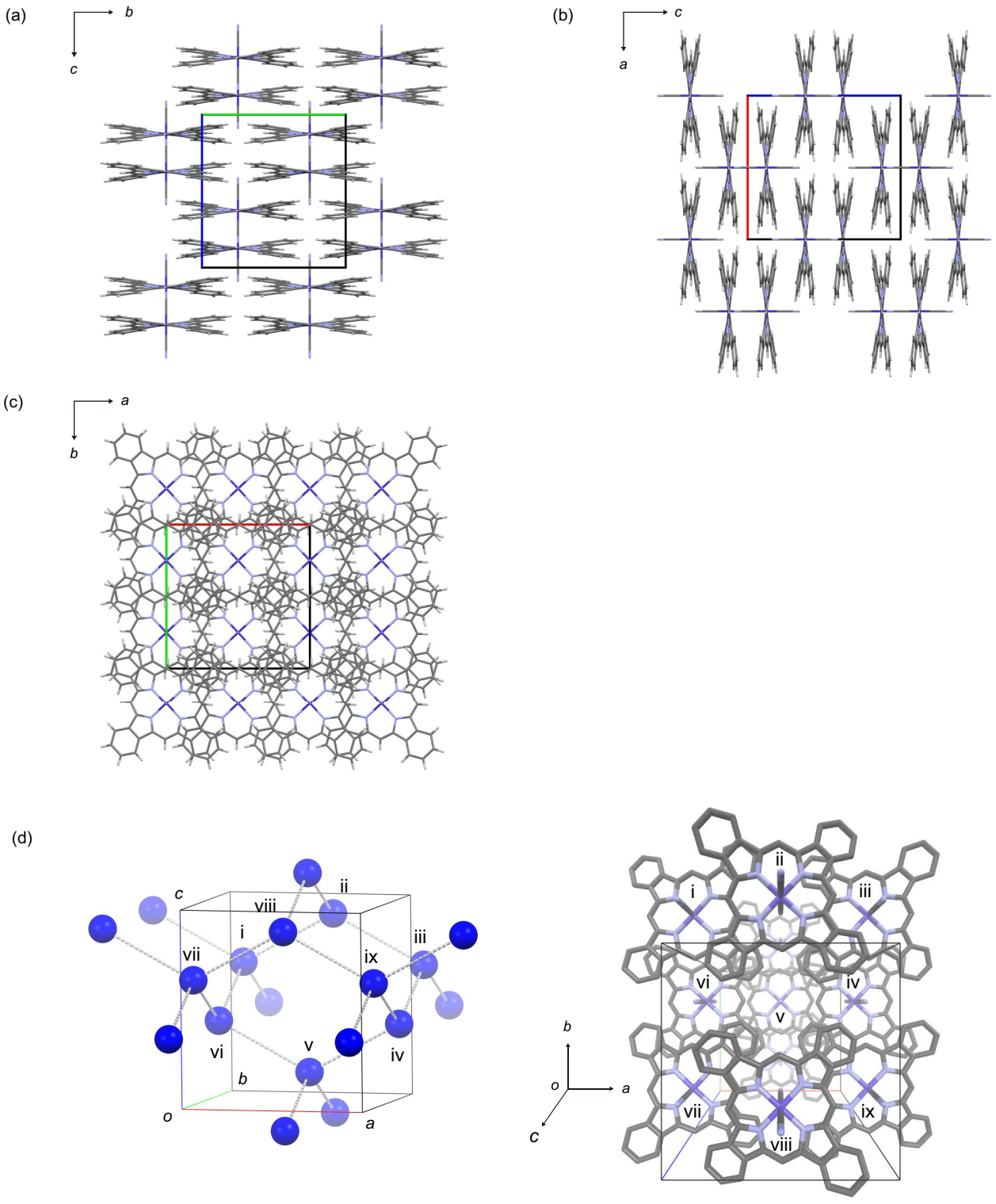


**Figure S3.** Crystal structure of Co(tbp)$(CN)_2$ viewed along the *a*-axis (a), *b*-axis (b), and *c*-axis (c), and (d) the diamond arrangement of Co atoms (left) in the crystal structure (right).

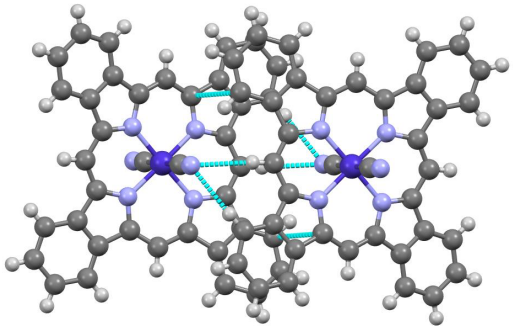

**Figure S4.** Intermolecular short contacts in $Co(tbp)(CN)_2$.

## References


1) a) S. Ito, T. Murashima, H. Uno, and N. Ono, *Chem. Commun.*, **1998**, 1661–1662; b) S. Ito, N. Ochi, T. Murashima, H. Uno, and N. Ono, *Heterocycles*, 2000, **52**, 399–411; c) S.-D. Jeong, B. Min, S. Y. Cho, C. Lee, B. K. Park, K.-S. An, and J. Lim, *J. Org. Chem.*, 2012, 77, 8329–8331.

2) G. M. Sheldrick, *Acta Crystallogr., Sect. A: Found. Adv.*, **2015**, *71*, 3–8.

3) G. M. Sheldrick, *Acta Crystallogr., Sect. C: Struct. Chem.*, **2015**, *71*, 3–8.

4) M. J. Frisch, G. W. Trucks, H. B. Schlegel, G. E. Scuseria, M. A. Robb, J. R. Cheeseman, G. Scalmani, V. Barone, G. A. Petersson, H. Nakatsuji, X. Li, M. Caricato, A. V. Marenich, J. Bloino, B. G. Janesko, R. Gomperts, B. Mennucci, H. P. Hratchian, J. V. Ortiz, A. F. Izmaylov, J. L. Sonnenberg, D. Williams-Young, F. Ding, F. Lipparini, F. Egidi, J. Goings, B. Peng, A. Petrone, T. Henderson, D. Ranasinghe, V. G. Zakrzewski, J. Gao, N. Rega, G. Zheng, W. Liang, M. Hada, M. Ehara, K. Toyota, R. Fukuda, J. Hasegawa, M. Ishida, T. Nakajima, Y. Honda, O. Kitao, H. Nakai, T. Vreven, K. Throssell, J. A. Montgomery, Jr., J. E. Peralta, F. Ogliaro, M. J. Bearpark, J. J. Heyd, E. N. Brothers, K. N. Kudin, V. N. Staroverov, T. A. Keith, R. Kobayashi, J. Normand, K. Raghavachari, A. P. Rendell, J. C. Burant, S. S. Iyengar, J. Tomasi, M. Cossi, J. M. Millam, M. Klene, C. Adamo, R. Cammi, J. W. Ochterski, R. L. Martin, K. Morokuma, O. Farkas, J. B. Foresman, and D. J. Fox, Gaussian 16, Revision A.03, Gaussian, Inc., Wallingford CT, 2016.